Journal of Magnetism and Magnetic Materials 413 (2016) 76–80

Contents lists available at ScienceDirect

Journal of Magnetism and Magnetic Materials

journal homepage: www.elsevier.com/locate/jmmm

Magnetic properties of point defects in proton irradiated diamond

T.N. Makgato [a,*], E. Sideras-Haddad [a,b], M.A. Ramos [c,d], M. García-Hernández [e], A. Climent-Font [c], A. Zucchiatti [c], A. Muñoz-Martin [c], S. Shrivastava [a], R. Erasmus [a,b]

[a] School of Physics, University of the Witwatersrand, Johannesburg 2050, South Africa
[b] Center of Excellence in Strong Materials, Physics Building, University of the Witwatersrand, Johannesburg 2050, South Africa
[c] CMAM, Centro de Micro-Analisis de Materiales, Universidad Autónoma de Madrid, C/Faraday 3, Campus de Cantoblanco, E-28049 Madrid, Spain
[d] Departamento de Fisica de la Materia Condensada, Condensed Matter Physics Center (IFIMAC) and Instituto Nicolás Cabrera, Universidad Autónoma de Madrid, 28049 Madrid, Spain
[e] Instituto de Ciencia de Materiales de Madrid, CSIC, Cantoblanco, E-28049 Madrid, Spain

ARTICLE INFO

Article history:
Received 18 January 2016
Received in revised form
7 April 2016
Accepted 14 April 2016
Available online 15 April 2016

Keywords:
Diamond
Proton irradiation
Paramagnetism
Superparamagnetism

ABSTRACT

We investigate the magnetic properties of ultra-pure type-IIa diamond following irradiation with proton beams of ≈ 1–2 MeV energy. SQUID magnetometry indicate the formation of Curie type paramagnetism according to the Curie law. Raman and Photoluminescence spectroscopy measurements show that the primary structural features created by proton irradiation are the centers: GR1, ND1, TR12 and 3H. The Stopping and Range of Ions in Matter (SRIM) Monte Carlo simulations together with SQUID observations show a strong correlation between vacancy production, proton fluence and the paramagnetic factor. At an average surface vacancy spacing of ≈ 1–1.6 nm and bulk (peak) vacancy spacing of ≈ 0.3-0.5 nm Curie paramagnetism is induced by formation of ND1 centres with an effective magnetic moment $\mu_{eff}\sim(0.1–0.2)\mu_B$. No evidence of long range magnetic ordering is observed in the temperature range 4.2-300 K.

1. Introduction

The realization of room temperature magnetic ordering in materials consisting purely of *sp* molecular orbitals promises leaps in science and could play a pivotal role in emerging technologies. However, in contrast to *d* and *f* electron materials from which standard magnetic devices are produced, these materials hardly occur naturally and despite numerous studies carried out to date, their fabrication by laboratory methods is not entirely understood and remains a field of intensive research. Earlier investigations on polymerized fullerenes [1,2] inspired more recent investigations [3–10] that indicate the presence of magnetically ordered states in purely *sp* electron based materials at room temperature. Of all *sp*-electron based materials, carbon materials are highly sought after due to the prospect of fabricating low cost, ultra-light, stable, durable and bio-compatible devices. In addition, carbon allotropes often feature extraordinary properties and have a substantially low spin-orbit coupling permitting long spin coherence times at room temperature (up to ∼ms for diamond [11]), an imperative for spin manipulation in emerging spin-based devices.

Diamond, an allotrope of carbon, has superior mechanical and thermal properties as well as a wide band gap (≈ 5.5 eV) which allows localized spins to be probed using microwave and optical frequencies for read-write applications of single photon sources in envisaged quantum computing devices [12]. Graphene on the other hand, is optically transparent and allows ballistic electron transport hence ultrafast carrier mobility leading to a variety of applications including high speed optical communications [13] and energy storage [14,15]. Localized magnetic states associated with zigzag edges in graphene nanoribbons exhibit intrinsically high spin wave stiffness, $D\sim2100$ meV/Å^2, higher than that of Fe and a corresponding spin correlation length ∼1 nm at room temperature [16]. The controlled production of room temperature ferromagnetism in carbon materials could therefore provide a means to achieve local control of both spin and electric charge using magnetic fields in conjunction with electromagnetic fields to produce devices capable of performing hybrid processing of quantum information [17].

To achieve these specialized applications material properties have to be tailored by modifying their physical properties. Ion implantation techniques have been instrumental in solid state materials modifications e.g. in the electronic doping of semiconducting materials [18–20] as it offers control in the introduction of point defects by means of defect concentration and implantation range. Using known simulation packages such as the Stopping and Range of Ions in Matter (SRIM) [21], estimates of radiation damage by vacancy production can be provided using readily available inputs such as ion energy, ion species, material composition and thickness.

* Corresponding author.
E-mail address: Thuto.Makgato@students.wits.ac.za (T.N. Makgato).

http://dx.doi.org/10.1016/j.jmmm.2016.04.030
0304-8853/

In this way the inter-vacancy spacing can be effectively controlled which is reported to be a critical parameter in triggering various forms of magnetism e.g. paramagnetism [22] and ferro (ferri) magnetism [23–25] in carbon systems.

In the present study, using specially made sample holders to minimize sample handling (contamination) and to ensure reproducibility in the measurements, we investigate the magnetic effects due to point defects introduced via proton irradiation at energies in the range $\approx$ 1–2 MeV in ultra-pure type IIa diamond.

2. Experimental details

Samples used in the present study are ultra-pure type IIa diamonds with nitrogen content 10-20 ppb as synthesized by Element Six using chemical vapour deposition (CVD) methods. Two samples (denoted A and B) of dimensions $\approx 4x4 \times 0.25$ mm^3 each were used. The samples were mounted using thermal varnish onto specially designed gold-coated quartz sample holders [26] that fit into both the irradiation target chamber as well as into the SQUID system for the propose of minimizing sample handling and ensuring reproducibility in measurements. Characterization of intrinsic and extrinsic defects was achieved by means of a commercial SQUID magnetometer from Quantum Design operated using the reciprocating sample option (RSO). The primary magnetic field was applied perpendicular to the $<001>$ crystallographic axes in all measurements. Both isomagnetic (with temperature cycled between 4.2 and 350 K) and isothermal (with the field cycled between ± 2 kOe) measurements were carried out. The sensitivity of the SQUID magnetometry system in RSO mode is enhanced from $\sim$1 μemu to $\sim$0.02 μemu and can thus adequately measure the effects of ion irradiation in the diamond samples. In all measurements, particular attention was applied to assess reproducibility and avoid incorporating common systematic artefacts.

Irradiation of the samples was carried out at room temperature using the 5 MV tandem accelerator of the Center of Micro-Analysis of Materials (CMAM) at the Universidad Autónoma de Madrid. The voltage at the accelerator terminal is regulated by a Cockcroft-Walton-type power supply, with a ripple of less than 50 V for a terminal voltage of 5 MV [26,27]. Fluence measurements are achieved by means of total charge integration during irradiation in an electrically isolated target chamber relative to ground. The diamond samples were irradiated at normal incidence (parallel to $<001>$ axes) using bulk proton beams of energies in the range 1.6–2.2 MeV and varying fluences (see Table 1). To simulate the kinetic effects of irradiation in diamond, we account for the radiation hardness of diamond by using a displacement energy of 45 eV [28,29] as an input in SRIM simulations which indicate that the maximum longitudinal range of protons is $\approx$ 29 μm from the irradiated surface of the samples and corresponds to the creation of $\approx$ 11 vacancies/ion.

Table 1
Summary of irradiation parameters utilized in the present investigation showing the energy, total ion fluence, longitudinal range and the number of vacancies produced per ion calculated using SRIM, respectively.

	E (MeV)	*F* (H$^+$/cm^2)	*R* (μm)	Vac/ion
A:I1	2.2	3.8×10^{17}	28.5	11.1
A:I2	2.0	7.1×10^{17}	24.3	10.7
A:I3	1.8	9.9×10^{17}	20.4	10.2
A:I4	1.6	12.4×10^{17}	16.9	9.8
B:I1	2.2	1.2×10^{18}	28.5	11.1
B:I2	2.2	2.2×10^{18}	28.5	11.1

Table 1 shows a summary of irradiation parameters utilized in the present investigation. The pristine (unirradiated) and irradiated samples A and B were further characterized using μ-Raman spectroscopy in which the 514 nm emission line from an argon laser is used in conjunction with a Horiba Jobin-Yvon LabRAM HR Raman spectrometer. The incident laser beam was focused onto the samples using the Olympus microscope attachment with a $100\times$ objective lens. The backscattered light was dispersed via a 600 lines/mm grating onto a liquid nitrogen-cooled charge coupled device (CCD) detector. Photoluminescence spectra spanning UV to near-Infra Red spectral frequencies were acquired using a $40\times$ UVB microscope objective lens from Thor Labs following electromagnetic excitation using a 244 nm UV probe. The behavior of point defects was further investigated following annealing of sample B at 800 °C in a hydrogen atmosphere for 120 min. SQUID and optical spectroscopy measurements (Raman and PL) were then carried out at room temperature to assess the effect of annealing in comparison to the pre-annealing data. SQUID measurements for sample A were acquired following the first irradiation (i.e. A: I1), the fourth irradiation (A: I4) and also after annealing (i.e. A: I4+Anneal). SQUID measurements for sample B were acquired following the first (B: I1) and the second irradiation, B: I2 (see Table 1).

3. Results and discussion

The pristine (unirradiated) diamond samples A and B both revealed a linear diamagnetic background that remains essentially invariant in the temperature range 4.2–300 K with magnetic susceptibility values of -4.8×10^{-7} emu/g and -5.0×10^{-7} emu/g respectively which are in close comparison with values reported in literature [30]. In both Fig. 1 and Fig. 2, the linear diamagnetic background contribution has been subtracted from the magnetic moment data to reveal the effects of irradiation. In Fig. 1, the acquired data follows an *s*-like curve behavior with saturation magnetization $\approx$ 0.5 μemu for sample A and $\approx$ 1.5 μemu for sample B at 300 K. A narrow hysteresis is observed (see Fig. 1 inset) with a remanence of $\approx$ 0.2 μemu and coercivity of 0.1 kOe indicating superparamagnetic (SPM) behavior both before and after irradiation at 300 K. The observed SPM originates from traces of ferromagnetic impurities in the diamonds such as Ni used as catalysts in the CVD diamond synthesis process.

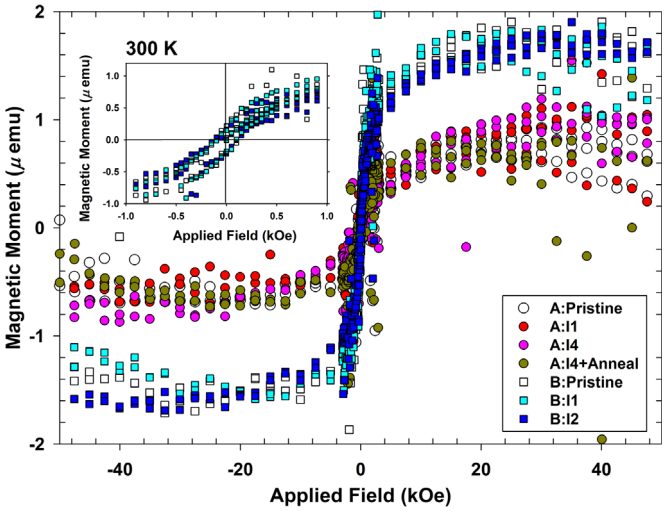

Fig. 1. Magnetic moments of diamond samples A and B acquired at different irradiation and annealing stages (see Table 1) as function of the applied field at 300 K.